



On the comparison among optimal measurement placement methods for a hybrid microgrid harmonic state estimation. Part II: numerical applications

关于混合微电网谐波状态估计的最佳测量选择方法之比较。第二部分：数值应用

L. Alfieri^{1*}, A. Bracale², P. De Falco¹, M. Aprea¹

¹Department of Electrical Engineering and of Information Technology, University of Naples Federico II, Naples - 80125, Italy

²Department of Engineering, University of Naples Parthenope, Naples - 80143, Italy

luisa.alfieri@unina.it

Accepted for publication on 12th October 2015

Abstract – This is a companion paper to the Part I paper, in which the theoretical aspects of the optimal measurement units (MUs) placement for the dynamic harmonic state estimation (DHSE) on a hybrid AC/DC micro grid (μ G) are analyzed. In particular, Part I dealt with two techniques, available in the relevant literature, for the optimal MUs placement; these techniques, based on the minimum condition number of the measurement matrix and on the integer linear programming, were properly used to obtain the measurements needed as inputs for the DHSE with a Kalman filter (KF). In this paper, numerical applications are presented, in order to compare the two methods in terms of: (i) number of required measurements to guarantee the observability of the system; (ii) the accuracy of the corresponding KF-based DHSE; (iii) computational burden. The numerical experiments were performed on a hybrid AC/DC μ G proposed for an actual industrial facility in southern Italy.

Keywords - Optimal measurement placement, dynamic harmonic state estimation, Kalman filter, micro grid, power quality.

I. INTRODUCTION

In the context of modern smart grids (SGs) and micro grids (μ Gs), the dynamic state estimation (DSE) is a concerning issue, since it was proved that it is a fundamental step for the optimal operation of the system [1-3]. The estimates of the state of the system are used as input data for different tasks; for example, to satisfy increasing needs in terms of required Power Quality (PQ) in the considered grid [4-5]. The PQ problem solution is of great interest in SGs and μ Gs, since specific PQ requirements must be verified for sensitive loads.

The aim of the companion paper [6] was to propose a method for the dynamic harmonic state estimation (DHSE) on

a hybrid AC/DC μ G, using a limited number of measurements as input data, in order to guarantee affordable installation and maintenance costs. The DHSE was performed through one of the most common methods proposed in the relevant literature [7]. In particular, the method proposed in [4], based on the Kalman filter (KF), was used.

In the companion paper [6] the measurements were properly selected using two techniques for the optimal measurement units (MUs) placement, available in literature [8-11]. Both techniques guarantee the observability of the system, and select the minimum number of MUs on the basis of the minimum condition number of the measurement matrix and on the basis of the integer linear programming approach, respectively. In this paper, numerical applications of the aforesaid placement methods were performed on an hybrid AC/DC μ G proposed for an actual industrial facility in southern Italy. First, a comparison between the two optimal MUs placement methods was performed on the basis of the number of required measurements and of the computational burden. Then, the selected measurements were used as input data for the KF-based DHSE, and a further comparison was performed in terms of estimates accuracy. The DHSE results were compared also with the results of a limit case in which all of the measurements were assumed to be available.

The remainder of this paper is organized as follows. In Section II a brief description of the hybrid AC/DC μ G is provided. In Section III the results of the optimal MUs placement methods are presented, while in Section IV the results of the KF-based DHSE are shown and discussed. Our conclusions are reported in Section V. In the Appendix, additional data about the analysed hybrid μ G are provided.

II. THE HYBRID AC/DC μ G

The optimal MUs placement procedures, shown in Section III of the companion paper [6], and the DHSE illustrated in

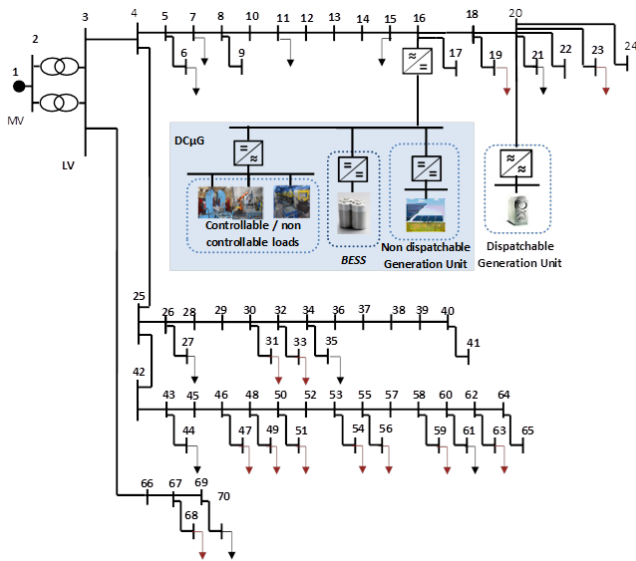


Fig. 1, Hybrid AC/DC μ G.

The μ G in Fig. 1 was proposed for an actual electrical distribution system of an industrial facility located in southern Italy. The original network is connected to the national MV distribution grid through two 630 kVA MV/LV transformers (20/0.4 kV), and includes four LV feeders, one for each different manufacturing process line. The total number N of buses is 70. The proposed AC/DC μ G includes three controllable loads, a PV generation plant, a gas micro turbine generator and a battery energy storage system (BESS). As shown in Fig. 1, an AC/DC static converter, placed in bus #16, connects the DC side to the AC side of the μ G; the micro turbine is located at bus #20. The red (black) arrows in Fig. 1 correspond to non-linear loads (linear loads). Tab.1 provides for non-linear loads (Tab. 1a) and linear loads (Tab. 1b): the bus allocation, the description of the industrial machine type, the rated power and the power factor.

Line parameters are reported in the Appendix. The hybrid μ G was simulated in MATLAB-Simulink environment, and the programs were developed and tested on a Windows PC with an Intel i7-3770 3.4 GHz and 16 GB of RAM. In the following, the results obtained by applying the proposed approaches are shown.

III. OPTIMAL MUS PLACEMENT METHODS

The optimal MUs placements obtained by using the minimum condition number method (MCNM) and the integer linear programming method (ILPM) are reported and compared with a limit case, in which all of the state variables are measured (AM).

Section IV of [6], were applied to the AC/DC hybrid μ G shown in Fig. 1.

With reference to the MCNM (Section 3.1 of the companion paper [6]), the measurement matrix for the fundamental component $\hat{H}(1)$ was determined from the admittance matrix $\hat{Y}_{NN}(1)$ and from the line-bus admittance matrix $\hat{Y}_{LN}(1)$, that can be both obtained from the knowledge of the equivalent circuit of the system.

TABLE 1, (A) NON-LINEAR LOADS; (B) LINEAR LOADS.

Bus	Type	Rated Power [kVA]	Power Factor
16	Sandblaster	55	0.75
16	Folding walls island robot	24	0.99
16	PLC + computer	3	0.62
19	Wave welding machine	30	0.65
23	Plasma cutting machine	15	0.8
31, 33	Core cutting machine n.1	60	0.8
47, 49, 51	MT winder machine	37	0.99
54, 56	Tuboly winder machine	37	0.99
59, 63	BT winder machine	37	0.99
68	Bender machine + robot	20	0.9

(A)

Bus	Type	Rated Power [kVA]	Power Factor
6	Painting machine	75	0.8
7	Box overturning machine	4	0.99
11	Welder aspirators	11	0.99
15	Manual bender	8	0.99
21	Corrugated walls machine	122	0.65
27	Crane	5.5	0.8
35	Autoclaves	86	0.8
44	Furnace	5	0.99
61	Offices	36	0.99
70	Testing bench room	50	0.7

(B)

With reference to the ILPM (Section 3.2 of the companion paper [6]), the binary transformation of the bus-bus admittance matrix into the connectivity matrix \mathbf{S} was performed, in order to define the constraints of the optimization problem. The weight factors w_i in the objective function were all assumed to be unitary. In fact, since there were no preferential buses for the MUs placement, the weight factors could be considered all equal.

The results of both methods, in terms of the minimum number of MUs to be installed and the number of state variables to be measured, are reported in Tab. 2, together with the data of the AM case.

Tab. 2 shows that both the MCNM and the ILPM require the same number of MUs to be installed, that is less than half of the maximum MUs number (AM case). Moreover, the ILPM requires the acquisition of a greater number of measurements than the MCNM, thus the MUs required in each case should be different in term of input channels. Note that the number of required line currents is the same for the MCNM and the ILPM, while the numbers of measured bus voltages and load currents are different.

Note that, as stated in Section 3.1 of the companion paper [6], the results of the MCNM in Tab. 2 were obtained considering only the measurement matrix for the fundamental component ($h = 1$). This choice was due to a preliminary sensitivity analysis, performed by considering each harmonic (including the fundamental component) separately and all harmonics together, as in [10]. Some results of the sensitivity analysis are reported in Tab. 3, on the basis of the number and the type of state variables to be measured.

From the analysis of Tab. 3 it is possible to note that, as the harmonic order h increases, the number of measured line currents and load currents decrease, while the number of measured bus voltages increases.

The MCNM, applied for all of the combined harmonic orders, requires the highest number of measurements, and therefore appears to be redundant to achieve the observability of the system. As shown in Section IV, the solution based on the fundamental component led to the best results in terms of estimates accuracy in our application.

Eventually, Tab. 4 shows the average computational time required by both the selected placement methods. It is clear that the ILPM requires the smallest amount of time to solve the optimization problem; the MCNM applied to fundamental component performs an iterative procedure for the reduction of the measurement matrix, and therefore is slower. In particular, the ILPM time is about 1/35 of the MCNM time.

TABLE 2, COMPARISON BETWEEN THE RESULTS OF THE OPTIMAL MUS PLACEMENT METHODS.

	Method		
	MCNM	ILPM	AM
Number of MUs	31	31	68
Number of measured line currents	60	60	68
Number of measured bus voltages	0	26	68
Number of measured load currents	8	0	68
Total number of measurements	68	86	204

TABLE 3, COMPARISON BETWEEN THE RESULTS OF THE MCNM FOR DIFFERENT HARMONIC ORDERS.

Selected harmonic order

	1-st	5-th	7-th	11-th	13-th	All
Number of measured line currents	60	13	11	1	1	60
Number of measured bus voltages	0	55	57	67	67	67
Number of measured load currents	8	0	0	0	0	8

TABLE 4, AVERAGE COMPUTATIONAL TIME OF THE SELECTED PLACEMENT METHODS.

	Method	
	MCNM	ILPM
Average computational time [s]	19.47	0.56

IV. DYNAMIC HARMONIC STATE ESTIMATION WITH KALMAN FILTER

The measurements taken through the MCNM, the ILPM and AM were separately considered as inputs for the KF-based DHSE. The DHSE, according to the model (17) of the companion paper [6], was performed to estimate the harmonic disturbances of order $h = 5, 7, 11, 13$, which usually are among the most significant disturbances in a distribution system. Measured and estimated disturbances in all of the buses where a non-linear load is placed were compared; however, for sake of conciseness, in this paper only the comparison of the disturbances in buses #23 and #54 are reported. Note that the harmonic disturbances, introduced in the μG by non-linear loads were directly measured from the original factory distribution system.

Note that buses #23 and #54 were selected since the corresponding load currents present different harmonic contents, so it is possible to evaluate the robustness of the KF-based DHSE on different load conditions. The spectra of the current waveforms at bus #23 and bus #54, are shown in Figs. 2a and 2b, respectively. These spectra were obtained by applying the Discrete Fourier Transform, according to the IEC standard [12-13].

From the analysis of Fig. 2, the differences in terms of harmonic components are evident. In particular, the most significant components of the spectrum in Fig. 2a are the 5-th, 7-th, 11-th and 13-th harmonics; therefore, the adopted model is consistent with the effective spectral content. On the other hand, the higher-order harmonics of the spectrum in Fig. 2b are not negligible, being their amplitudes of the same order of magnitude of the 11-th and 13-th harmonics; therefore, the model used to represent the disturbances appears incomplete.

The estimates of the waveforms at buses #23 and #54, obtained with the KF-based DHSE coupled to the MCNM, the ILPM and AM are shown in Figs. 3a-4a, 3b-4b and 3c-4c,

respectively. The analysis of Figs. 3 and 4 reveals that KF estimates with the MCNM are better than KF estimates with the ILPM. This difference is magnified when an incomplete disturbance model is used (Fig. 4) since the results obtained with the ILPM are significantly poorer than the results obtained with the MCNM. A different behaviour is detected also for AM, which provides the best results when the disturbance model is incomplete (Fig. 4c); this could be due to the corrective effect of all of the measurements taken from the μ G. On the other hand, when the model properly fits the measured waveform, the presence of all of the measurements may cause a worsening effect on the aggregate estimates (Fig. 3c).

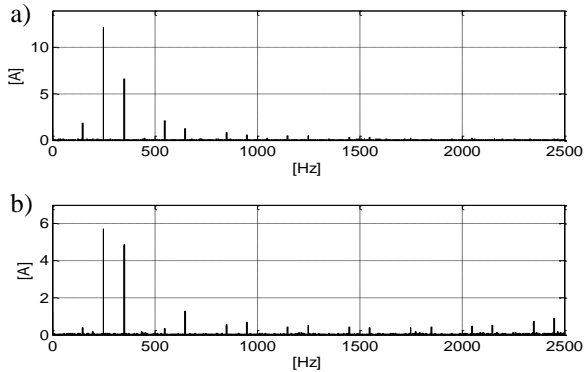


Fig. 2, Spectra of the current waveforms deprived of the fundamental component. Bus #23 (a); Bus #54 (b).

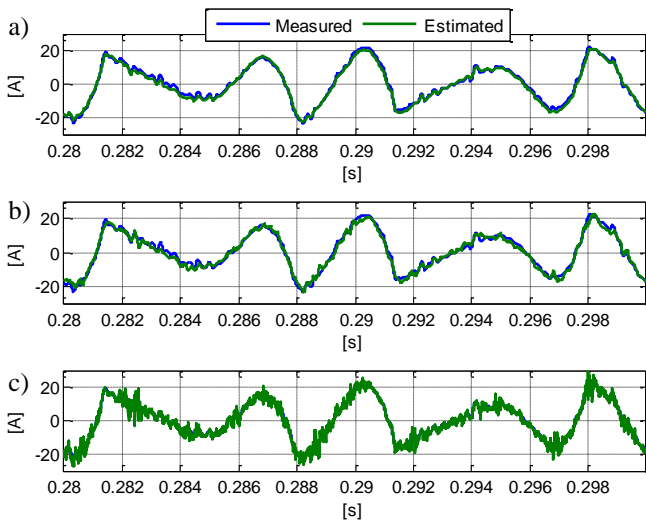


Fig. 3, Bus #23: comparison between actual and estimated current waveforms. KF combined to (a) MCNM, (b) ILPM, (c) AM.

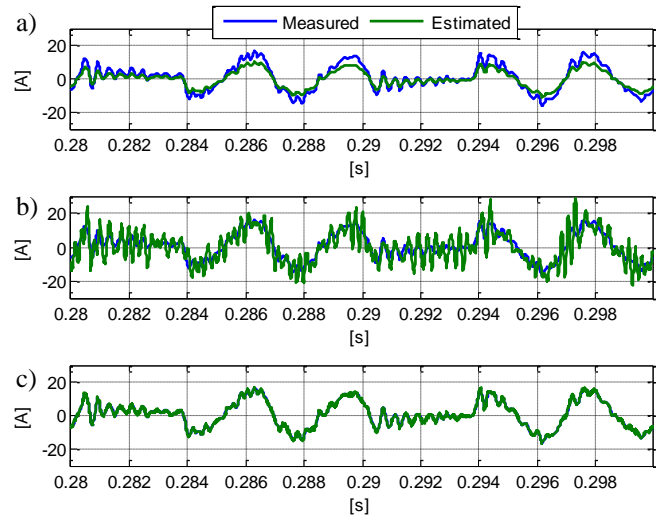


Fig. 4, Bus #54: comparison between actual and estimated current waveforms. KF combined to (a) MCNM, (b) ILPM, (c) AM.

For sake of completeness, Tab. 5 shows the percentage reconstruction errors, related to the waveforms in Figs. 3 and 4, calculated as $e_{\%} = \frac{1}{N} \sum_i \left| \frac{x_i - \hat{x}_i}{x_{max}} \right| \cdot 100$, where x is the measured disturbance vector, \hat{x} is the estimated disturbance vector and x_{max} is the maximum value of x . From the analysis of Tab. 5, it clearly appears that the errors on the aggregate estimates at bus #23 with the MCNM and the ILPM are comparable; instead, the ILPM error at bus #54 is almost double than the MCNM error. The AM error is greater than both MCNM and ILPM errors at bus #23, while it is significantly lower than them (about 1/6 and 1/11, respectively) at bus #54.

TABLE 5, PERCENTAGE RECONSTRUCTION ERRORS

Method	$e_{\%}$	
	Bus #23	Bus #54
KF with MCNM	4.45	13.86
KF with ILPM	5.99	27.09
KF with AM	7.22	2.45

A further comparison between the results of the KF-based DHSE was effected in terms of reconstruction error for each harmonic order that was considered in the model. For sake of conciseness, in Tab. 6 only the reconstruction errors related to the harmonic components of the disturbance in the bus #23 are reported. From the analysis of these values, it can be noted that for both KF with the ILPM and KF with the MCNM the reconstruction errors increase as the harmonic order increases, since the amplitude of the harmonic component decreases, as shown in Fig. 2a. In particular, KF with the ILPM provides the least accurate estimates of each harmonic component, while KF with the MCNM appears to be the best solution for the DHSE. KF with AM supplies accurate estimates at each harmonic, although it provided the worst aggregate waveform estimate, as reported in Tab. 5. This was due to the introduction of high-frequency components during the

dynamic estimation, as shown in Fig. 3c; these high-frequency components obviously affect the aggregate reconstruction error, but do not invalidate the single harmonic estimates.

TABLE 6, COMPARISON BETWEEN THE ERROR

	$e_{\%}$			
	5-th	7-th	11-th	13-th
KF with MCNM	0.11	0.30	0.35	0.81
KF with ILPM	1.72	5.97	8.79	14.73
KF with AM	0.74	0.99	0.31	1.49

Finally, the sensitivity analysis on the performances of the MCNM for different harmonic orders (including the fundamental component), and for all of the combined harmonic orders, was performed on the basis of the corresponding DHSE accuracy, as previously evidenced. For sake of conciseness, only the comparison between the results obtained applying MCNM at the 1-st and 7-th harmonic orders, and for all of the combined harmonic orders are shown in Tab. 7, for both the previously considered buses.

From the analysis of the reconstruction errors in Tab. 7, the DHSE with the measurements provided by the MCNM at the fundamental component seems to be the most reliable, since it shows the best performances when the disturbance is well-modelled (bus #23), and it still shows a satisfying accuracy when the disturbance is not well-modelled (bus #54). Moreover, for the disturbance at bus #54, we note that the error of the DHSE with the MCNM at all of the combined harmonic orders is similar to the error of the DHSE with the MCNM at the fundamental component. For the disturbance at bus #23, the error of the DHSE with the MCNM at all of the combined harmonic orders increases significantly, although the global number of measurements increases. This is coherent with the results obtained in Tab.5 for the AM case. On the other hand, the results obtained by MCNM at the 7-th harmonic seem to be globally inaccurate.

TABLE 7, COMPARISON OF THE RESULTS OF THE MCNM, FOR DIFFERENT HARMONIC ORDERS, IN TERMS OF DHSE ACCURACY

Selected harmonic order	$e_{\%}$	
	Bus #23	Bus #54
1-st	4.45	13.86
7-th	7.99	42.20
All	20.96	13.47

V. CONCLUSIONS

This paper provides an application of the DHSE on a hybrid AC/DC μ Gs. The DHSE is performed through a KF-based approach. The necessary measurements required in the KF are obtained from MUs, which have been placed on the basis of the results of two optimal placement methods, commonly used for AC networks: the minimum condition number method and the integer linear programming method.

The performances of each placement method and of the correspondent DHSE were compared in terms of: (i) number of required measurements to guarantee the observability of the system; (ii) accuracy of the corresponding KF-based DHSE; (iii) computational burden. Moreover, a limit case, in which the measurements of all of the state variables were available, was also considered.

The methods were tested on a hybrid AC/DC μ G proposed for an actual industrial facility located in southern Italy. The numerical applications showed that the results obtained by using the measurements provided by the MCNM as input data for the DHSE were generally better than the results obtained with the measurement provided by ILPM. Moreover, both methods allowed a reliable DHSE in presence of a reduced number of measurements, thus reducing the total costs for the installation of MUs. In terms of computational burden, MNCM appeared more onerous than ILPM.

APPENDIX

In the following, the data of the lines of the hybrid AC/DC μ G are provided. Specifically, for each line, the starting and ending buses, the length, the resistance and the reactance per unit length are shown in Tabs. 8, 9, 10, 11.

TABLE 8, LINE PARAMETERS FOR THE FIRST FEEDER OF THE PLANT

Buses		ℓ [m]	R [m Ω /m]	X [m Ω /m]
from	to			
3	4	8	0.041	0.014
4	5	24	0.163	0.130
5	6	4	0.473	0.101
5	7	0.5	0.163	0.130
7	8	6	0.163	0.130
8	9	10	1.410	0.112
8	10	9.3	0.163	0.130
10	11	3	0.163	0.130
11	12	2.8	0.163	0.130
12	13	3.5	0.163	0.130
13	14	3.5	0.163	0.130
14	15	11	0.163	0.130
15	16	19.1	0.163	0.130
16	17	4	1.410	0.112
16	18	1.9	0.163	0.130
18	19	4	1.410	0.112
18	20	3	0.163	0.130
20	21	10	0.236	0.097
20	22	42	1.410	0.112
20	23	61	2.240	0.119
20	24	61	1.410	0.112

TABLE 11, LINE PARAMETERS FOR THE FOURTH FEEDER OF THE PLANT

Buses		ℓ [m]	R [mΩ/m]	X [mΩ/m]
From	to			
2	66	30	0.094	0.090
66	67	87	0.163	0.130
67	68	7	1.410	0.112
67	69	0.5	0.163	0.130
69	70	7	0.473	0.101

TABLE 9, LINE PARAMETERS FOR THE SECOND FEEDER OF THE PLANT

Buses		ℓ [m]	R [mΩ/m]	X [mΩ/m]
from	to			
4	25	31	0.041	0.014
25	26	3.5	0.163	0.130
26	27	16	2.240	0.119
26	28	9	0.163	0.130
28	29	12.5	0.163	0.130
29	30	10.5	0.163	0.130
30	31	8	0.641	0.101
30	32	1.5	0.163	0.130
32	33	10	0.641	0.101
32	34	12.5	0.163	0.130
34	35	8	0.328	0.096
34	36	13	0.163	0.130
36	37	1	0.163	0.130
37	38	35	0.665	0.260
38	39	0.5	0.665	0.260
39	40	0.5	0.665	0.260
40	41	20	1.410	0.112

TABLE 10, LINE PARAMETERS FOR THE THIRD FEEDER OF THE PLANT

Buses		ℓ [m]	R [mΩ/m]	X [mΩ/m]
From	to			
25	42	34	0.041	0.014
42	43	3.3	0.070	0.096
43	44	12	2.240	0.119
43	45	9.2	0.070	0.096
45	46	5.5	0.070	0.096
46	47	5.5	1.410	0.112
46	48	6.5	0.070	0.096
48	49	5.5	1.410	0.112
48	50	7.8	0.070	0.096
50	51	5.5	1.410	0.112
50	52	5.2	0.070	0.096
52	53	1.8	0.070	0.096
53	54	5.5	1.410	0.112
53	55	8.1	0.070	0.096
55	56	5.5	1.410	0.112
55	57	5.6	0.070	0.096
57	58	4.5	0.070	0.096
58	59	5.5	1.410	0.112
58	60	3	0.070	0.096
60	61	8	0.473	0.101
60	62	2.5	0.070	0.096
62	63	5.5	1.410	0.112
62	64	3.7	0.070	0.096
64	65	38	1.410	0.112

ACKNOWLEDGMENTS

This work was supported by Ministero dell'Istruzione dell'Università e della Ricerca (MIUR) in the frame of PON03PE_00178_1: Microgrid Ibride in Corrente Continua e Corrente Alternata (MICCA). The authors also thank Prof. Guido Carpinelli for his constructive support in the realization of this work.

REFERENCES

- [1] A. Jain, and N.R. Shivakumar. "Impact of PMU in dynamic state estimation of power systems," *Power Symposium, 2008. NAPS '08. 40th North American*, vol., no., pp.1,8, 28-30 Sept. 2008
- [2] N.R. Shivakumar, and A. Jain. "A Review of Power System Dynamic State Estimation Techniques," *Joint International Conference on Power System Technology and IEEE Power India Conference, POWERCON 2008.*, Oct. 12—15, 2008
- [3] E. Ghahremani, and I. Kamwa. "Dynamic State Estimation in Power System by Applying the Extended Kalman Filter With Unknown Inputs to Phasor Measurements," *IEEE Transactions on Power Systems*, **26**, pp. 2556-2566, 2011
- [4] A. Griffio, G. Carpinelli, D. Lauria, and A. Russo. "An optimal control strategy for power quality enhancement in a competitive environment," *International Journal of Electrical Power & Energy Systems*, **29**, pp. 514-525, 2007
- [5] P.T. Baboli, M. Shahparasti, and M.P. Moghaddam, M.R. Haghifam, M. Mohamadian, "Energy management and operation modeling of hybrid AC-DC microgrid," *IET Generation, Transmission & Distribution*, **8**, pp. 1700-1711, 2014
- [6] L. Alfieri, A. Bracale, P. De Falco, and M. Aprea. "On the comparison among optimal measurement placement methods for a hybrid micro grid harmonic state estimation. Part I: Theoretical Aspects," in *Proceedings of 3rd International Symposium on Energy Challenges and Mechanics*, Aberdeen, Scotland, UK, July 7-9, 2015
- [7] U. Arumugam, N. M. Nor, and M. F. Abdullah, "A Brief Review on Advances of Harmonic State Estimation Techniques in Power Systems," *International Journal of Information and Electronics Engineering*, **1**, pp. 217-222, 2011

- [8] W. Yuill, A. Edwards, S. Chowdhury, and S.P. Chowdhury, "Optimal PMU placement: A comprehensive literature review," *Power and Energy Society General Meeting, 2011 IEEE*, July 24–29, 2011
- [9] K.K. More, H.T. Jadhav. "A literature review on optimal placement of phasor measurement units," *International Conference on Power, Energy and Control (ICPEC)*, pp. 220-224, Feb. 6–8, 2013
- [10] C. Madtharad, S. Premrudeepreechacharn, N.R. Watson, and Ratchai Saeng-Udom. "An optimal measurement placement method for power system harmonic state estimation," *IEEE Transactions on Power Delivery*, **20**, pp. 1514-1521, 2005
- [11] B. Xu, and A. Abur. "Observability analysis and measurement placement for system with PMUs," in *Proc. IEEE Power System Conf. Expo.*, **2**, pp. 943-946, 2004
- [12] *Testing and measurement techniques – Power quality measurement methods*. IEC standard 61000-4-30, 2008
- [13] *General guide on harmonics and interharmonics measurements, for power supply systems and equipment connected thereto*. IEC standard 61000-4-7, 2009